



# $^{18}\text{F}$ -Fluoride Positron Emission Tomography and Positron Emission Tomography/Computed Tomography

Einat Even-Sapir, MD, PhD,\* Eyal Mishani, PhD,<sup>†</sup> Gideon Flusser, MD,<sup>‡</sup> and Ur Metser, MD\*

$^{18}\text{F}$ -Fluoride is a positron-emitting bone-seeking agent, the uptake of which reflects blood flow and remodeling of bone. Assessment of  $^{18}\text{F}$ -fluoride kinetics using quantitative positron emission tomography (PET) methods allows the regional characterization of lesions of metabolic bone diseases and the monitoring of their response to therapy. It also enables the assessment of bone viability and discrimination of uneventful and impaired healing processes of fractures, bone grafts and osteonecrosis. Taking advantage of the favorable pharmacokinetic properties of the tracer combined with the high performance of PET technology, static  $^{18}\text{F}$ -fluoride PET is a highly sensitive imaging modality for detection of benign and malignant osseous abnormalities. Although  $^{18}\text{F}$ -fluoride uptake mechanism corresponds to osteoblastic activity, it is also sensitive for detection of lytic and early marrow-based metastases, by identifying their accompanying reactive osteoblastic changes, even when minimal. The instant fusion of increased  $^{18}\text{F}$ -fluoride uptake with morphological data of computed tomography (CT) using hybrid PET/CT systems improves the specificity of  $^{18}\text{F}$ -fluoride PET in cancer patients by accurately differentiating between benign and malignant sites of uptake. The results of a few recent publications suggest that  $^{18}\text{F}$ -fluoride PET/CT is a valuable modality in the diagnosis of pathological osseous conditions in patients also referred for nononcologic indications.  $^{18}\text{F}$ -fluoride PET and PET/CT are, however, not widely used in clinical practice. The limited availability of  $^{18}\text{F}$ -fluoride and of PET and PET/CT systems is a major factor. At present, there are not enough data on the cost-effectiveness of  $^{18}\text{F}$ -fluoride PET/CT. However, it has been stated by some experts that  $^{18}\text{F}$ -fluoride PET/CT is expected to replace  $^{99\text{m}}\text{Tc}$ -MDP bone scintigraphy in the future. Semin Nucl Med 37:462-469 © 2007 Elsevier Inc. All rights reserved.

$^{18}\text{F}$ -Fluoride is a positron-emitting bone-seeking agent with favorable pharmacokinetic properties that was introduced by Blau and coworkers in 1962.<sup>1-5</sup> Its uptake mechanism resembles that of  $^{99\text{m}}\text{Tc}$ -MDP. After intravenous administration,  $^{18}\text{F}$ -fluoride diffuses through the bone capillaries into the bone extracellular fluid (ECF). Its plasma clearance is more rapid than that of  $^{99\text{m}}\text{Tc}$ -MDP, and its single-passage extraction efficiency is higher because of its

smaller molecular weight and the fact that its protein binding is negligible whereas binding of  $^{99\text{m}}\text{Tc}$ -MDP to plasma proteins varies from 25% after injection to 70%, 12 hours after injection. In the blood, approximately 30% of  $^{18}\text{F}$ -fluoride is transported by erythrocytes. The single-pass extraction of  $^{18}\text{F}$ -fluoride is, however, almost 100% as the red blood cell  $^{18}\text{F}$ -fluoride, is available for clearance to bone.<sup>5-7</sup> The fast blood clearance of  $^{18}\text{F}$ -fluoride results in a better target-to-background ratio. From the bone ECF,  $^{18}\text{F}$ -fluoride ions exchange with hydroxyl groups in the hydroxyapatite at the surface of bone crystals forming fluoroapatite mainly at sites of bone remodeling with high turnover.<sup>1</sup> Therefore, uptake of  $^{18}\text{F}$ -fluoride reflects blood flow and osteoblastic activity. Bone uptake of  $^{18}\text{F}$ -fluoride is 2-fold greater than that of  $^{99\text{m}}\text{Tc}$ -MDP.<sup>2,8,9</sup>

Combining the favorable pharmacokinetic characteristics of  $^{18}\text{F}$ -fluoride with the high performance of positron emission tomography (PET) technology,  $^{18}\text{F}$ -fluoride is a valuable imaging modality of the skeleton. Quantitative methods of

\*Department of Nuclear Medicine, Osteoradiology Unit, Tel-Aviv Sourasky Medical Center, Sackler Faculty of Medicine, Tel-Aviv University, Tel-Aviv, Israel.

<sup>†</sup>The Cyclotron Unit, Hadassah-Hebrew University Medical Center, Jerusalem, Israel.

<sup>‡</sup>Department of Radiology, Osteoradiology Unit, Tel-Aviv Sourasky Medical Center, Sackler Faculty of Medicine, Tel-Aviv University, Tel-Aviv, Israel.

Address reprint requests to Einat Even-Sapir, MD, PhD, Department of Nuclear Medicine, Tel-Aviv Sourasky Medical Center, 6 Weizman Street, Tel-Aviv 64239, Israel. E-mail: evensap@tasmc.health.gov.il

<sup>18</sup>F-fluoride PET imaging allow dynamic measurement of the tracer uptake and regional characterization of metabolic bone lesions, monitoring their response to therapy, and separation between uneventful and impaired healing processes of bone fracture, osteonecrosis and graft incorporation.<sup>10-26</sup> Static <sup>18</sup>F-fluoride PET is highly sensitive for detection of malignant and benign bone abnormalities.<sup>27-45</sup> As various pathological bone conditions are associated with increased uptake of <sup>18</sup>F-fluoride, PET findings often require morphological characterization for accurate diagnosis. This is now easily achieved by using hybrid PET/computed tomography (CT) systems.<sup>36,37,41,43</sup>

## **<sup>18</sup>F-Fluoride PET/CT: Technical Notes**

### **<sup>18</sup>F-Fluoride Preparation**

<sup>18</sup>F-Fluoride was produced by the <sup>18</sup>O(p,n)<sup>18</sup>F nuclear reaction in 2 mL of enriched <sup>18</sup>O water as a target and then transferred into a fluorination module by a flow of argon. After trapping, it was loaded on an anion exchange column, dried, eluted with 1 mL of K<sub>2</sub>CO<sub>3</sub> solution (5 mg/mL), and transferred to the reactor. After the addition of 1 mL of sterile water, the solution was heated to 120°C (2 minutes), followed by evaporation under reduced pressure. After the temperature of the solution was lowered to 30°C, 10 mL of saline and 4 mL of phosphate buffer (ph = 7) were added and transferred into a product vial through a 0.22- $\mu$  sterile filter. Chemical and radiochemical purity were analyzed by anion exchange high-performance liquid chromatography on an IC-PAKTM anion HR (4.6\*75 mm, Waters) and eluted with sodium borate/gluconate solution and acetonitrile (20 mL borate gluconate concentrate, 20 mL n-butanol, 120 mL acetonitrile, and 860 mL deionized water) at a flow of 0.8 mL/min.<sup>36</sup>

### **PET/CT Imaging**

No special preparations are needed before the performance of <sup>18</sup>F-fluoride PET/CT study. In most centers, scanning takes place approximately 60 minutes after injection. High-quality PET images can be acquired, however, within a very wide time-interval from 30 minutes to 4 hours after injection. The <sup>18</sup>F-fluoride administered dose is usually 370 MBq (10 mCi). To reduce the radiation dose, mainly in patients referred for nononcologic indications, it is possible to inject only 185 MBq (5 mCi) of <sup>18</sup>F-fluoride and increase acquisition time, maintaining the high quality of the images. The CT can be a full-dose CT or, as used in our center, reduced-dose CT with 140 kV, 80 mA, 0.8 seconds per CT rotation, a pitch of 6, and a table speed of 22.5 mm/s, without any specific breath-holding instructions. A PET emission scan is performed immediately after the acquisition of CT, without changing the patient's positioning. A total of 5 to 9 bed positions are performed with acquisition time of 3 minutes for each one (5 minutes when administered dose has been reduced), imaging the skeleton from skull to femurs. If lesions are suspected to be located at the distal peripheral bones, PET/CT acquisition

includes these areas.<sup>36,41</sup> In addition to morphological data, the CT part of the study is used for attenuation correction. The need to perform attenuation correction in <sup>18</sup>F-fluoride PET is yet to be determined. Tayama and coworkers<sup>46</sup> calculated bone-to-muscle ratios for <sup>18</sup>F-fluoride PET images with and without attenuation correction. Their conclusion was that attenuation correction is not necessary for accurate visual interpretation of <sup>18</sup>F-fluoride PET images. Lim and coworkers<sup>44</sup> assessed the role of <sup>18</sup>F-fluoride PET in young patients with back pain. In some cases, high tracer uptake in the renal collecting systems led to streak artifacts in the reconstructed PET images, which caused low tracer uptake and poor visualization of the adjacent spine. In these cases, calculated attenuation correction eliminated the artifact. The latter correction can be applied retrospectively.

### **Radiation Exposure**

Radiation exposure of <sup>18</sup>F-fluoride resembles that of <sup>99m</sup>Tc-MDP. Injection of 185 MBq (5 mCi) <sup>18</sup>F-fluoride in an adult patient is associated with effective dose of 4.25 mGy, which is comparable with 4.75 mGy when 740 MBq (20 mCi) of <sup>99m</sup>Tc-MDP is injected.<sup>44,47,48</sup> Although in oncologic patients CT is a routine imaging procedure, the additional radiation exposure of CT should be considered with caution in patients who are referred for nononcologic indications. The CT acquisition protocol used in our department is associated with radiation exposure of 7.3 mGy in an adult patient and 10.5 mGy in a 10-year-old-patient. Reduction from 140 kV to 120 kV may achieve reduction in radiation exposure to 5.1 mGy and 7.35 mGy, respectively, and reduction of mAs to 40 may result in exposure of the child to 3.7 mGy.<sup>48</sup> It is also possible to alter the workflow so that, instead of whole-body CT, only regional CT will be added after PET, based on the scintigraphic findings.

### **Quantitative**

#### **Assessment of <sup>18</sup>F-Fluoride Uptake**

Quantitative assessment of <sup>18</sup>F-fluoride uptake and its change over time has been used for assessment of normal bone physiology, characterization of bone pathology, and monitoring response to therapy. A method for assessing the full kinetics of <sup>18</sup>F-fluoride has been described by Hawkins and coworkers. The technique is a nonlinear regression (NLR) method composed of 3 compartments, and 4 rate constants.<sup>3</sup> With this technique, data are obtained by combing dynamic PET acquisition and arterial blood sampling. The 3 compartments are plasma, bone ECF, and bone mineral. The 4 rate contrasts are  $k_1$  clearance of <sup>18</sup>F-fluoride from the plasma to the total bone,  $k_2$  reverse transfer from the ECF to plasma,  $k_3$  incorporation of <sup>18</sup>F-fluoride into the bone mineral, and  $k_4$  release of <sup>18</sup>F-fluoride from the mineral.  $K_i$  calculated as  $(k_1 \times k_3) / (k_2 + k_3)$  is the net uptake of <sup>18</sup>F-fluoride to bone mineral. The parameters obtained by the NLR method were found by Piert and coworkers in porcine model to correlate with histomorphologic findings of bone formation.<sup>18</sup> As an alternative to NLR method,  $K_i$  can be estimated by Patlak graphical analysis, which applies to the linear part of the time-activity

curve. It can be performed more easily and robustly than NLR method but still, it requires blood sampling and dynamic PET imaging and therefore is also not used on a regular basis.<sup>49</sup> Standardized uptake value (SUV), which averages tracer uptake with respect to the injected dose and body weight, is the most widely used PET index for assessment of tracer uptake in routine clinical practice because it does not require blood sampling and is obtained by static PET acquisition. SUV was found to correlate with the full kinetic <sup>18</sup>F-fluoride modeling in both normal and pathological bone and can therefore substitute NLR and Patlak analysis, although one should keep in mind that SUV may be less reliable, particularly in areas with low metabolic activity, such as the long bones of the peripheral skeleton.<sup>50</sup>

There is a large variability in the normal values of <sup>18</sup>F-fluoride uptake in different skeletal regions. The highest values are found in trabecular bones, as in the vertebrae, characterized by greater bone turnover compared with long bones of the peripheral skeleton, which are predominately cortical.<sup>4,15,16,24</sup>

## The Clinical Role of <sup>18</sup>F-Fluoride Imaging

### Assessment of Metabolic Bone Diseases and Other Pathological Bone Conditions Using Quantitative <sup>18</sup>F-Fluoride Imaging

In vivo assessment of <sup>18</sup>F-fluoride kinetics allows characterization of bone disease as well as monitoring response to therapy. Specific regions in the skeleton can be individually assessed. This section will address the clinical role of quantitative <sup>18</sup>F-fluoride PET.

### Metabolic Bone Disease: Paget, Osteoporosis, and Renal Osteodystrophy

Several groups have investigated the kinetics of <sup>18</sup>F-fluoride in Paget's disease.<sup>19,24</sup> In Pagetic bones,  $K_1$  values were increased more than 3-fold and  $k_1$  values were increased more than 2-fold, reflecting increased regional bone formation and plasma clearance to the total bone, respectively.<sup>19,24</sup> The value of  $k_2$  was reported to be lower in Pagetic bones, perhaps as result of the fact that the marrow is often replaced by fibrous tissue and therefore <sup>18</sup>F-fluoride is less available for return to plasma. The value of  $k_4$  was also found lower in Pagetic bones, suggesting that <sup>18</sup>F-fluoride is more tightly bound to bone.<sup>24</sup> Characterizing the kinetics of <sup>18</sup>F-fluoride allows objective monitoring of the response of Paget therapy. Blockers of bone remodeling, the biphosphonates, are currently used for treatment of patients with Paget's disease. A month after initiation of therapy, Installe and coworkers observed a decrease in  $K_1$  and  $k_1$  values, although <sup>18</sup>F-fluoride uptake remained greater than in normal bone. Six months after successful treatment, there was a further decrease in <sup>18</sup>F-fluoride uptake, and  $k_1$  values reached those values measured in normal bones. There was no significant change in  $k_2$ ,  $k_3$ , and  $k_4$  values. Nonresponse was associated

with no change in  $K_1$  values and an increase in SUV. These findings suggest that the decrease of <sup>18</sup>F-fluoride in Pagetic bones after treatment with biphosphonates is related to decrease in the clearance of <sup>18</sup>F-fluoride from the blood to bone, although mineralization may remain unaffected. Although full kinetic evaluation is more accurate, it appears that SUV measured 60 minutes after injection may be suitable for monitoring the response of Pagetic bones to therapy and separation between responders and nonresponders in clinical practice. Clinical assessment of the response to biphosphonates therapy relies on measurement of blood and urine markers of bone resorption and formation. This approach may be of limited value in monostotic disease. When comparing the change in <sup>18</sup>F-fluoride uptake with biochemical markers during treatment, the latter were found to normalize a month after initiation of therapy whereas <sup>18</sup>F-fluoride uptake remained high in Pagetic bones. It is yet to be seen, however, whether this discrepancy has any practical implication on treatment approach.<sup>24</sup>

Cook and coworkers investigated the regional differences in <sup>18</sup>F-fluoride kinetics between lumbar vertebrae and the humerus of postmenopausal women using the NLR 3-compartmental modeling. Mean vertebral values were significantly greater than humeral  $K_1$  values. These observations allow a better understanding of the differences in the pathophysiology of metabolic impairment in different skeletal regions consisting of different bone type (trabecular or cortical), as well as the regional difference in response to treatment.<sup>16</sup> In another study by this group, the regional skeletal kinetics measured by dynamic <sup>18</sup>F-fluoride PET and biochemical markers of bone formation and resorption, were measured in 72 postmenopausal women classified as normal, osteopenic, or osteoporotic according to bone mineral densitometric score at the lumbar spine. Lower values of  $K_1$  were found in women classified as osteoporotic, whereas levels of bone-specific alkaline phosphatase, a measure of global bone formation, were significantly increased indicating that in postmenopausal osteoporosis, the global skeletal bone turnover is increased whereas the regional bone formation at the lumbar spine composed of predominately trabecular bone, is reduced.<sup>20</sup>

Monitoring the response to antiresorptive therapy by the quantitation of <sup>18</sup>F-fluoride uptake also was found valuable in osteoporosis. High values of  $K_1$  and  $k_1$  were found in both juvenile and postmenopausal osteoporosis.<sup>4,15</sup> Measuring the change in bone metabolism and blood flow by <sup>18</sup>F-fluoride PET of the lumbar spine after Risedronate therapy, Frost and coworkers found successful response to be associated with decrease in  $K_1$  values and decrease in  $k_2$  values, suggesting an increase in the reverse transfer of <sup>18</sup>F-fluoride from the bone ECF to the blood and decrease in  $k_3/(k_2 + k_3)$ , indicating a decrease in the fraction of tracer found in the ECF, which undergoes specific binding to the bone matrix.<sup>15</sup>

When performed in patients with renal osteodystrophy, quantitative <sup>18</sup>F-fluoride assessment separated lesions with low turnover from lesions of secondary hyperparathyroidism, which showed greater  $K_1$  values. These values decreased when patients underwent parathyroidectomy.<sup>10</sup>

## **Bone Grafts, Healing Fractures, and Osteonecrosis**

<sup>18</sup>F-fluoride uptake is a valuable diagnostic tool for assessment of the viability of bone grafts, early prediction of fracture nonunion and diagnosis of osteonecrosis. Brenner and coworkers have performed serial <sup>18</sup>F-fluoride imaging in 34 patients with cancellous and full bone grafts. In general, both types of grafts showed decrease in uptake 2 years after surgery but uptake was still significantly higher in cancellous grafts and in the border zone of full bone grafts compared with normal limb bones. The time-course of changes in metabolism reflected by the change in uptake values measured at different time points was different for the two graft types. Although cancellous grafts were characterized by a stepwise decrease in bone metabolism, full-bone grafts have showed initial increase in <sup>18</sup>F-fluoride uptake with a subsequent decrease. In cancellous grafts, the decrease in <sup>18</sup>F-fluoride uptake between 6 to 24 months after surgery, correlated with a relatively fast healing of the small bone chips with formation of stable union within a year after surgery. In full bone grafts, healing is usually delayed and complications and nonunion tend to occur more frequently being diagnosed clinically and radiologically as late as 18-24 months after surgery. There is agreement between <sup>18</sup>F-fluoride uptake of different parts of full-bone grafts and the histopathologic findings in the corresponding areas. In the contact zones, histopathologic assessment shows ongoing graft remodeling up to 48 months after surgery and correspondingly, <sup>18</sup>F-fluoride uptake increases reaching a peak at about one year after surgery with subsequently decreasing bone activity. In contrast, the central parts of full-bone grafts show no remodeling and low <sup>18</sup>F-fluoride uptake. Nonunion of the graft, which requires surgical intervention is characterized by increased <sup>18</sup>F-fluoride uptake reflecting the ongoing repair mechanisms which involves increased blood flow, vascular permeability, and high bone turnover.<sup>23</sup>

Piert and coworkers observed a prolonged increased bone <sup>18</sup>F-fluoride uptake in patients after hip augmentation surgery with allogenic acetabular grafts compared with genuine cortical bone. Their hypothesis was that the increased bone metabolism in allogenic bone graft was caused by a reduced ability to respond to the same extent as genuine bone to increased metabolic demands after surgery, with continuous stress to the normal surrounding bone, which corresponded with histopathologic findings of prolonged new bone formation in peripheral areas.<sup>13</sup>

In a small number of patients, the quantitation of <sup>18</sup>F-fluoride uptake has been used for evaluation of new bone formation around a femoral allograft inserted for treatment of prosthetic loosening. During the first year, uptake was increased. It decreased to that measured in the contralateral femur when measured 6 years after successful surgery.<sup>26</sup> In another pilot study, 8 patients who underwent anterior cruciate ligament reconstruction by incorporation of a tendon graft in a bone tunnel underwent quantitative <sup>18</sup>F-fluoride PET to follow the regional bone turnover starting a day after surgery until 22 months later. The highest uptake value was

measured 3 weeks after surgery and remained high until 7 months after surgery. It was almost normal at 22 months after surgery.<sup>25</sup> Quantitative <sup>18</sup>F-fluoride PET imaging also has been used for the assessment of perfusion and osteoblastic activity of revascularized fibular grafts for mandibular reconstruction. The technique was found valuable in separating between uneventful graft healing, early failure and nonunion.<sup>11,14,21</sup>

Early diagnosis of delayed union or nonunion of fractures is a challenging imaging task. Such diagnosis by conventional imaging is still suboptimal resulting in delay in 9 to 12 months with a consequent poor outcome. Serial plain radiographs are being used to follow callus formation. CT allows one to reconstruct bony architecture in 3-dimensions. However, both modalities detect mineralized bone formation, which is the late manifestation of the fracture healing process. Magnetic resonance imaging (MRI) is a valuable diagnostic tool for the assessment of fracture healing, although it is less sensitive in identifying impaired fracture healing when located in long bones. The role of quantitative <sup>18</sup>F-fluoride PET in early identification of impaired fracture healing was investigated in rat model by Hsu and coworkers. Although the union site was characterized by a progressive increase in uptake up to the 3-week time point and then stabilization, only minimal uptake was constantly observed in impaired healing. These findings suggest that <sup>18</sup>F-fluoride PET can potentially predict the development fracture nonunion earlier than other imaging techniques.<sup>22</sup> The role of <sup>18</sup>F-fluoride PET in this clinical setting in humans is, however, yet to be determined.

Osteonecrosis of the femoral head may be a serious complication of fracture, treatment with high-dose steroids, or idiopathic treatment. In a pilot study in 5 patients with osteonecrosis, quantitative <sup>18</sup>F-fluoride PET was found valuable for in vivo assessment of the regional blood supply of the femoral head as well as in monitoring the changes over time and prediction of outcome.<sup>12</sup>

## **Detection of Malignant and Benign Lesions by Static <sup>18</sup>F-Fluoride PET and PET/CT**

<sup>18</sup>F-fluoride PET is the most sensitive imaging modality for detection of malignant bone involvement.<sup>27-42</sup> The regional clearance of <sup>18</sup>F fluoride from plasma to bone is 3-fold or greater in metastatic lesions than in normal bone.<sup>3</sup> Schirmermeister and coworkers have shown, in several reports, the superiority of <sup>18</sup>F-fluoride-PET for the detection of metastatic skeletal involvement compared with <sup>99m</sup>Tc-MDP bone scintigraphy (BS).<sup>29,30,32,35</sup> In 34 patients with breast cancer, <sup>18</sup>F-fluoride PET identified the presence of small bone marrow metastases.<sup>30</sup> In a prospective study in 53 patients with small cell lung cancer or locally advanced nonsmall-cell lung cancer, the detection of bone metastases by planar BS, SPECT of the vertebral column, and <sup>18</sup>F-fluoride PET were compared. Sensitivity of the 3 modalities was 78%, 94%, and 99%, respectively. Scintigraphic findings were associated

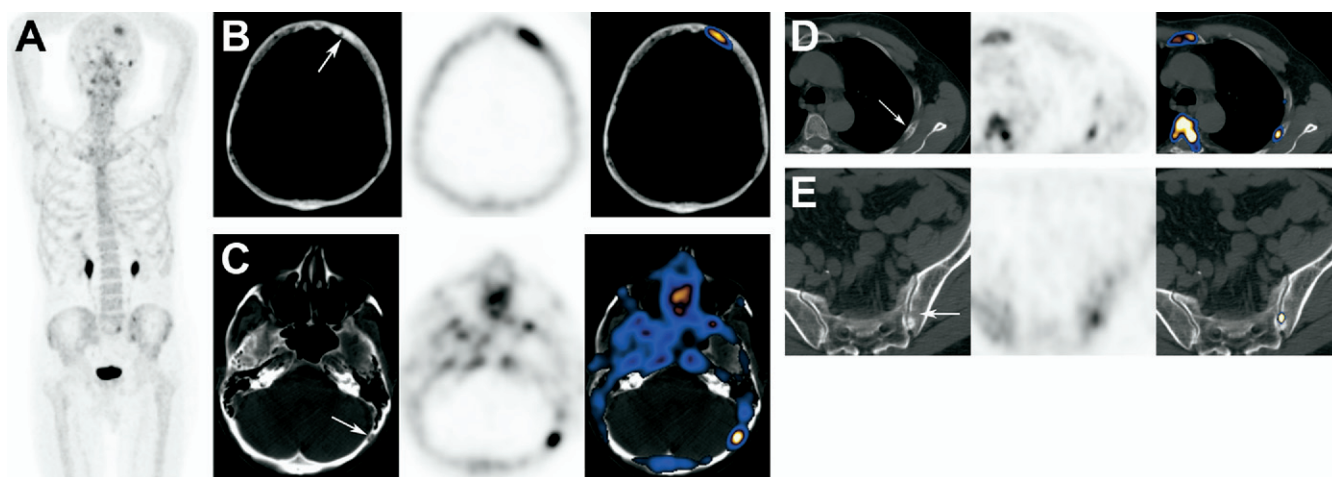


**Figure 1** Early metastatic spread of prostate cancer. Shown is a 72-year-old patient with high-risk prostate cancer. Based on  $^{18}\text{F}$ -fluoride PET/CT findings, early skeletal metastatic spread was diagnosed, altering the patient's treatment approach from regional to systemic. The malignant lesions are subtle on CT and were overlooked when CT was interpreted alone but were identified when fused with PET data. (A) MIP image, (B-E) metastases pointed by arrows. Each row represents, from left to right, CT, PET, and fused PET/CT data of a metastasis, noted by an arrow. (B) Increased uptake in the left skull with corresponding sclerotic changes is shown. Lytic-type metastases in the skull (C), rib (D), and left pelvis (E) are shown. Of note is a nonspecific sclerotic lesion in the left pelvis, which does not show increased uptake, whereas anterior to it there is a very subtle lytic lesion reflected as noncontinuity of the bone cortex with focal increased uptake. Although the former is not a metastasis, the latter is.

with change in patient management in 9% of patients based on SPECT findings and in 11% of patients based on the findings of  $^{18}\text{F}$ -fluoride PET.<sup>32</sup>

However,  $^{18}\text{F}$ -fluoride is not tumor-specific and also accumulates excessively in benign bone abnormalities. As a matter of fact, because of its high sensitivity,  $^{18}\text{F}$ -fluoride PET performed for assessment of malignant bone involvement is prone to a high rate of false-positive interpretations by detecting nonmalignant lesions, including lesions that are usually not detected with  $^{99\text{m}}\text{Tc}$ -MDP-BS, such as uncomplicated small cysts.<sup>21,36</sup> It is not possible to differentiate benign from malignant lesions based on the intensity of  $^{18}\text{F}$ -fluoride uptake.<sup>33</sup> Lesions detected on  $^{18}\text{F}$ -fluoride PET, therefore, often require correlation with CT and/or MRI.<sup>21</sup> The use of hybrid PET/CT has improved significantly the limited specificity of  $^{18}\text{F}$ -fluoride PET because the morphologic CT appearance of the scintigraphic lesion achieves accurate differentiation between benign lesions and metastases. To evaluate the diagnostic accuracy of  $^{18}\text{F}$ -fluoride PET/CT in assessing malignant osseous involvement and in differentiating malignant from benign bone lesions, we performed  $^{18}\text{F}$ -fluoride PET/CT studies in 44 cancer patients and found a statistically significant improvement in the specificity of  $^{18}\text{F}$ -fluoride PET/CT (97%) compared with  $^{18}\text{F}$ -fluoride-PET alone (72%) on a lesion-based analysis and 88% versus 56% on a patient-based analysis.<sup>36</sup> In another study in a more selective patient population, high-risk prostate cancer patients, we compared the detection of bone metastases by planar BS, multifield of view SPECT of the axial skeleton,  $^{18}\text{F}$ -fluoride PET, and  $^{18}\text{F}$ -fluoride PET/CT.  $^{18}\text{F}$ -Fluoride PET/CT was statistically more sensitive and more specific than planar and/or SPECT BS and more specific than  $^{18}\text{F}$ -fluoride PET. On a patient-based anal-

ysis, the sensitivity of planar BS, SPECT and  $^{18}\text{F}$ -fluoride was 70%, 92% 100%, respectively. Specificity of planar BS, SPECT,  $^{18}\text{F}$ -fluoride PET, and  $^{18}\text{F}$ -fluoride PET/CT was 57%, 82%, 62%, and 100%.<sup>41</sup>

On fused images of PET/CT, the morphology of all lesions showing increased  $^{18}\text{F}$ -fluoride uptake is instantly provided. Although  $^{18}\text{F}$ -fluoride uptake mechanism corresponds to osteoblastic activity, it is highly sensitive for detection of lytic and early marrow-based metastases and not only osteoblastic ones (Figs. 1 and 2). The reactive osteoblastic activity, which accompanies lytic lesions and malignant marrow deposits, is reflected by increased uptake of  $^{18}\text{F}$ -fluoride in the periphery of the lesions, even when minimal.<sup>27,30,36,37</sup> As illustrated in Fig. 2,  $^{18}\text{F}$ -fluoride PET/CT also is valuable for the assessment of malignant bone involvement in oncologic diseases with predominately intramedullary and lytic bone lesions such as multiple myeloma. PET/CT images allow a direct comparison between the diagnostic accuracy of  $^{18}\text{F}$ -fluoride PET and that of CT.  $^{18}\text{F}$ -Fluoride PET appears to be more sensitive in detecting bone abnormalities. Of 111 metastases identified by increased  $^{18}\text{F}$ -Fluoride uptake, the appearance of bone CT was normal in 16 (14%).<sup>36</sup> PET/CT is beneficial in ruling out metastatic spread when nonspecific lesions are reported on CT. In patients with prostate cancer, a tumor type with predominately osteoblastic metastases, the presence of nonspecific sclerotic lesions on CT pose dilemma as they may represent metastatic spread or be bone islands with no clinical relevance. Although the former show increased  $^{18}\text{F}$ -fluoride, the latter lesions are negative on PET (Fig. 1).<sup>41</sup>

Most data on the role of  $^{18}\text{F}$ -fluoride PET in benign conditions address the use of quantitative PET and evaluation of  $^{18}\text{F}$ -fluoride kinetics. There are only few studies on the role of

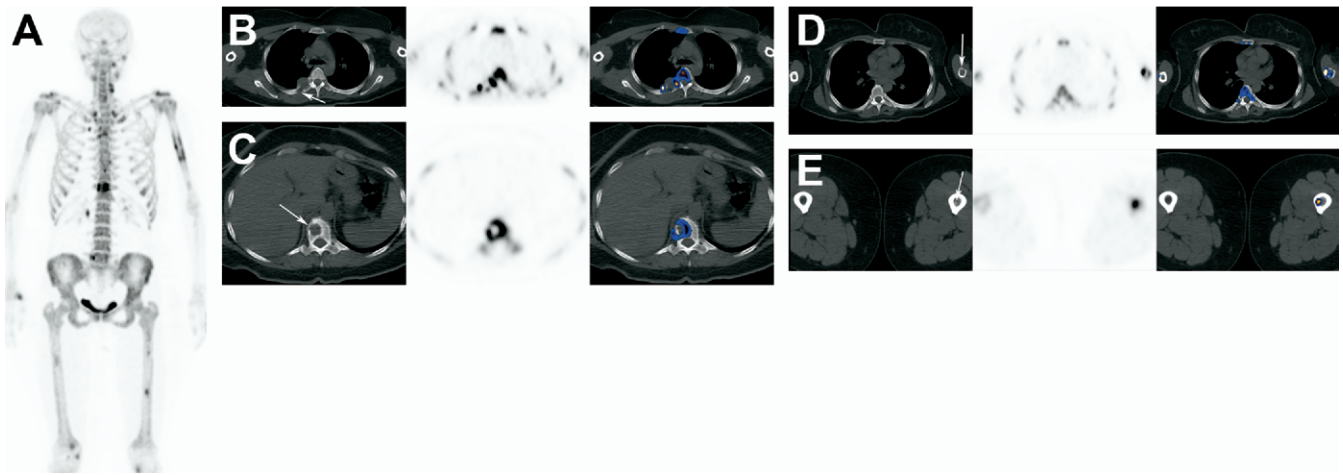


**Figure 2** Multiple myeloma. Shown is a 54-year-old female patient with multiple myeloma. (A) MIP image. Before <sup>18</sup>F-fluoride PET/CT imaging, she had known lesions only in a rib (B) and in a vertebra (C). <sup>18</sup>F-fluoride PET/CT identified multiple unexpected lesions. Two such lesions located in the left humerus are presented, lytic (D), and intramedullary (E). Each row represents, from left to right, CT, PET, and fused PET/CT data of a myeloma lesion, noted by an arrow.

static <sup>18</sup>F-fluoride PET for the detection of lesions in patients referred for nononcologic indications. With the evolving use of PET and PET/CT technology in routine clinical practice, data on the clinical use of <sup>18</sup>F-fluoride for detection of benign bone abnormalities are being accumulated. In a pilot study in a small group of patients with painful knee after arthroplasty, <sup>18</sup>F-fluoride PET was found valuable in detecting aseptic loosening and differentiating loosening from simple synovitis.<sup>45</sup> Two manuscripts were published recently on the role of <sup>18</sup>F-fluoride imaging in assessment of back pain in children and young adults, one using PET and the other using hybrid PET/CT.<sup>43,44</sup> Performance of <sup>18</sup>F-fluoride PET/CT in this clinical setting allowed accurate diagnosis of various etiologies of

back pain including pars interarticularis stress, spinous process injury, sacroiliac joint inflammation or stress, and osteoid osteoma. An important observation was the high negative predictive value of a normal study. Patients who had a negative <sup>18</sup>F-fluoride PET/CT did not need any medical intervention and the pain resolved spontaneously.<sup>43</sup>

We have performed <sup>18</sup>F-fluoride PET/CT in 82 patients referred for nononcologic indications, including acute back pain (n = 36), chronic back pain (n = 18), hip joint pain (n = 16), acute knee pain (n = 6), assessment of vertebral fusion mass (n = 3), and assessment of the viability of free fibular flaps (n = 3) (unpublished data). The instant fusion of scintigraphic findings with CT was beneficial in body regions

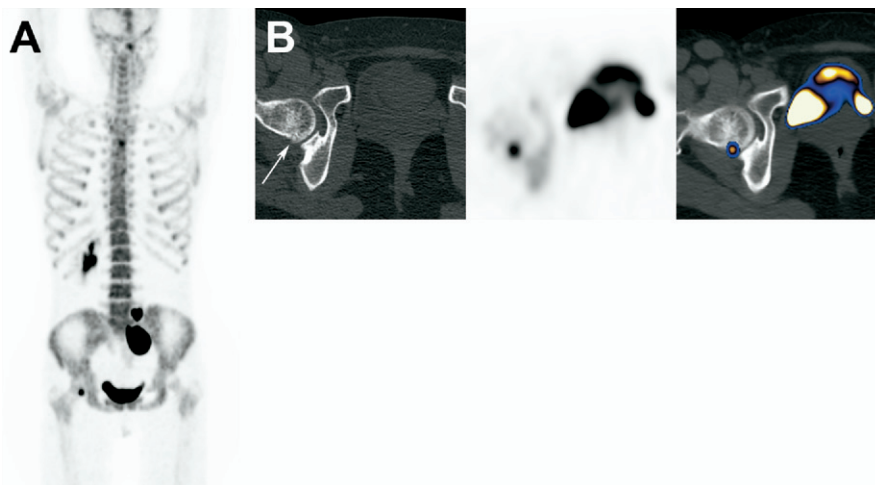


**Figure 3** Osteoid osteoma. A 24-year-old female patient with severe right hip joint pain and negative conventional imaging workup is shown. (A) MIP image. (B) Focal increased uptake of <sup>18</sup>F-fluoride is detected in the periphery of the left femur found to correspond in location with a small osteoid osteoma (arrow). From left to right, CT, PET, and fused PET/CT data are illustrated. This abnormality was overlooked when CT was read alone. The patient underwent successful radiofrequency ablation. The uptake seen in the left pelvis is radioactive urine in the collecting system of a pelvic kidney.



**Figure 4** Facet joint disease and inactive pars defect. Shown is a 32-year-old female patient with acute back pain. Before undergoing  $^{18}\text{F}$ -fluoride PET/CT imaging, she was diagnosed with bilateral L5 pars defects, which was thought to be the cause for her symptoms. (A) MIP image. (B) The increased uptake appears to be located in degenerative facet changes of L3 on the right (arrow). (C) The known defects on both sides of L5 show no increased uptake in keeping with inactive defects (arrows).

with a complicated 3-dimensional structure such as the hip joint and allowed the identification of relevant lesions, which were overlooked when CT was interpreted alone (Fig. 3). In some cases, bone abnormality suggested by CT to cause the patient symptoms was negative on PET, whereas other relevant lesion associated with increased  $^{18}\text{F}$ -fluoride uptake was identified (Fig. 4).

Despite the high performance of  $^{18}\text{F}$ -fluoride PET/CT, it is not widely used. The tracer is not always commercially available, and the number of PET/CT systems is smaller than the number of gamma cameras.  $^{18}\text{F}$ -fluoride PET or PET/CT is reserved for selected patients, either high-risk cancer patients or patients who are suspected clinically to have malignant or benign skeletal problems even though conventional imaging modalities and/or BS are negative or nonconclusive. It has been stated already by some authors that  $^{18}\text{F}$ -fluoride imaging is expected to replace bone scintigraphy completely within several years.<sup>40</sup> However, the decision to use of  $^{18}\text{F}$ -fluoride PET or PET/CT routinely warrants meticulous cost-effectiveness analysis. In a report by Hetzel and coworkers on 103 patients with lung cancer, the cost-effectiveness of  $^{18}\text{F}$ -fluoride PET was compared with that of bone scintigraphy with SPECT of the spine.  $^{18}\text{F}$ -fluoride PET was found more effective than planar and SPECT BS but was associated with higher incremental costs.<sup>35</sup> There are no data on the cost effectiveness of  $^{18}\text{F}$ -fluoride PET/CT. Such analysis should compare the cost-effectiveness of PET/CT to separate performance of BS and correlative CT, which at present, is the commonly applied imaging algorithm in patients with suspected bone abnormality.

## References

- Blau M, Nagler W, Bender MA: A new isotope for bone scanning. *J Nucl Med* 3:332-334, 1962
- Blau M, Ganatra R, Bender MA:  $^{18}\text{F}$ -fluoride for bone imaging. *Semin Nucl Med* 2:31-37, 1972
- Hawkins RA, Choi Y, Huang SC, et al: Evaluation of skeletal kinetics of fluorine 18-fluoride ion and PET. *J Nucl Med* 33:633-642, 1992
- Schiepers C, Nuyts J, Bormans G, et al: Fluoride kinetics of the axial skeleton measured in vivo with fluorine-18-fluoride PET. *J Nucl Med* 38:1970-1976, 1997
- Blake GM, Park-Holoan SJ, Cook GJR, et al: Quantitative studies of bone with the use of F18-fluoride and Tc99m-methylene diphosphate. *Semin Nucl Med* 1:28-49, 2001
- Wootton R, Dore C: The single-passage extraction of  $^{18}\text{F}$  in rabbit bone. *Clin Physiol Meas* 7:333-343, 1986
- Hoh CK, Hawkins RA, Dahlbom M, et al: Whole body skeletal imaging with ( $^{18}\text{F}$ ) fluoride ion and PET. *J Comput Assist Tomogr* 17:34-41, 1993
- Toegel S, Hoffmann O, Wadsak W, et al: Uptake of bone-seekers is solely associated with mineralization. A study with  $^{99\text{m}}\text{Tc}$ -MDP,  $^{153}\text{Sm}$ -EDTMP and  $^{18}\text{F}$ -fluoride on osteoblasts. *Eur J Nucl Med Mol Imaging* 33:491-494, 2006
- Ishiguro K, Nakagaki H, Tsuboi S, et al: Distribution of fluoride in cortical bone of human rib. *Calcif Tissue Int* 52:278-282, 1993
- Messa C, Goodman WG, Hoh CK, et al: Bone metabolic activity measured with positron emission tomography and [ $^{18}\text{F}$ ]fluoride ion in renal osteodystrophy: correlation with bone histomorphometry. *J Clin Endocrinol Metab* 77:949-955, 1993
- Berding G, Burchert W, van den Hoff J, et al: Evaluation of the incorporation of bone grafts used in maxillofacial surgery with [ $^{18}\text{F}$ ]fluoride ion and dynamic positron emission tomography. *Eur J Nucl Med* 22: 1133-1140, 1995
- Schiepers C, Broos P, Miserez M, et al: Measurement of skeletal flow with positron emission tomography and  $^{18}\text{F}$ -fluoride in femoral head osteonecrosis. *Arch Orthop Trauma Surg* 118:131-135, 1998
- Piert M, Winter E, Becker GA, et al: Allogenic bone graft viability after hip revision arthroplasty assessed by dynamic [ $^{18}\text{F}$ ]fluoride ion positron emission tomography. *Eur J Nucl Med* 26:615-624, 1999
- Schliephake H, Berding G, Knapp WH, et al: Monitoring of graft perfusion and osteoblast activity in revascularised fibula segments using [ $^{18}\text{F}$ ]-positron emission tomography. *Int J Oral Maxillofac Surg* 28: 349-355, 1999
- Frost ML, Cook GJ, Blake GM, et al: A prospective study of risedronate on regional bone metabolism and blood flow at the lumbar spine measured by  $^{18}\text{F}$ -fluoride positron emission tomography. *J Bone Miner Res* 18:2215-2222, 2003

16. Cook GJ, Lodge MA, Blake GM, et al: Differences in skeletal kinetics between vertebral and humeral bone measured by <sup>18</sup>F-fluoride positron emission tomography in postmenopausal women. *J Bone Miner Res* 15:763-769, 2000
17. Forrest N, Welch A, Murray AD, et al: Emoral head viability after Birmingham resurfacing hip arthroplasty: Assessment with use of [<sup>18</sup>F] fluoride positron emission tomography. *J Bone Joint Surg Am* 88:84-89, 2006 (Suppl)
18. Piert M, Zittel TT, Becker GA, et al: Assessment of porcine bone metabolism by dynamic [<sup>18</sup>F]fluoride ion PET: Correlation with bone histomorphometry. *J Nucl Med* 42:1091-1100, 2001
19. Cook GJ, Blake GM, Marsden PK, et al: Quantification of skeletal kinetic indices in Paget's disease using dynamic <sup>18</sup>F-fluoride positron emission tomography. *J Bone Miner Res* 17:854-859, 2002
20. Frost ML, Fogelman I, Blake GM, et al: Dissociation between global markers of bone formation and direct measurement of spinal bone formation in osteoporosis. *J Bone Miner Res* 19:1797-1804, 2004
21. Berding G, Schliephake H, van den Hoff J, et al: Assessment of the incorporation of revascularized fibula grafts used for mandibular reconstruction with F-18-PET. *Nuklearmedizin* 40:51-58, 2001
22. Hsu WK, Feeley BT, Krenek L, et al: The use of (18)F-fluoride and (18)F-FDG PET scans to assess fracture healing in a rat femur model. *Eur J Nucl Med Mol Imaging*, in press
23. Brenner W, Vernon C, Conrad EU, et al: Assessment of the metabolic activity of bone grafts with (18)F-fluoride PET. *Eur J Nucl Med Mol Imaging* 31:1291-1298, 2004
24. Installé J, Nzeusseu A, Bol A, et al: (18)F-fluoride PET for monitoring therapeutic response in Paget's disease of bone. *J Nucl Med* 46:1650-1658, 2005
25. Sörensen J, Michaelsson K, Strand H, et al: Long-standing increased bone turnover at the fixation points after anterior cruciate ligament reconstruction: A positron emission tomography (PET) study of 8 patients. *Acta Orthop* 77:921-925, 2006
26. Ullmark G, Sörensen J, Långström B, et al: Bone regeneration 6 years after impaction bone grafting: A PET analysis. *Acta Orthop* 78:201-205, 2007
27. Petren-Mallmin M, Andrasson I, Ljunggren O, et al: Skeletal metastases from breast cancer: Uptake of F18-fluoride measured with positron emission tomography in correlation with CT. *Skelet Radiol* 27:72-76, 1998
28. Hoegerle S, Juengling F, Otte A, et al: Combined FDG and F-18-fluoride whole body PET: A feasible two-in-one approach to cancer imaging. *Radiology* 209:253-258, 1998
29. Schirrmeyer H, Guhlmann A, Elsner K, et al: Sensitivity in detecting osseous lesions depends on anatomic localization: Planar bone scintigraphy versus <sup>18</sup>F PET. *J Nucl Med* 40:1623-1629, 1999
30. Schirrmeyer H, Guhnamm A, Kotzerke J, et al: Early detection and accurate description of extent of metastatic bone disease in breast cancer with fluoride ion and positron emission tomography. *J Clin Oncol* 17:2381-2389, 1999
31. Cook GJ, Fogelman I: The role of positron emission tomography in the management of bone metastases. *Cancer* 88:2927-2933, 2000
32. Schirrmeyer H, Glatting G, Hetzel J, et al: Prospective evaluation of clinical value of planar bone scan, SPECT and <sup>18</sup>F-labeled NaF PET in newly diagnosed lung cancer. *J Nucl Med* 42:1800-1804, 2001
33. Cook GJ, Fogelman I: The role of positron emission tomography in skeletal disease. *Semin Nucl Med* 3:50-61, 2001
34. Wahl RL: Current status of PET in breast cancer imaging, staging, and therapy. *Semin Roentgenol* 36:250-260, 2001
35. Hetzel M, Arslanemir C, König HH, et al: F-18 NaF PET for detection of bone metastases in lung cancer: Accuracy, cost-effectiveness, and impact on patient management. *J Bone Miner Res* 18:2206-2214, 2003
36. Even-Sapir E, Metser U, Flusser G, et al: Assessment of malignant skeletal disease with <sup>18</sup>F-Fluoride PET/CT. *J Nucl Med* 45:272-278, 2004
37. Even-Sapir E: Imaging of malignant bone involvement by morphologic, scintigraphic, and hybrid modalities. *J Nucl Med* 46:1356-1367, 2005
38. Eubank WB, Mankoff DA: Current and future uses of positron emission tomography in breast cancer imaging. *Semin Nucl Med* 34:224-240, 2004
39. Schoder H, Larson SM: Positron emission tomography for prostate, bladder, and renal cancer. *Semin Nucl Med* 34:274-292, 2004
40. Fogelman I, Cook G, Israel O, Van der Wall H: Positron emission tomography and bone metastases. *Semin Nucl Med* 35:135-142, 2005
41. Even-Sapir E, Metser U, Mishani E, et al: The detection of bone metastases in patients with high-risk prostate cancer: <sup>99m</sup>Tc-MDP planar bone scintigraphy, single- and multi-field-of-view SPECT, <sup>18</sup>F-fluoride PET, and <sup>18</sup>F-fluoride PET/CT. *J Nucl Med* 47:287-297, 2006
42. Langsteiger W, Heinisch M, Fogelman I: The role of fluorodeoxyglucose, <sup>18</sup>F-dihydroxyphenylalanine, <sup>18</sup>F-choline, and <sup>18</sup>F-fluoride in bone imaging with emphasis on prostate and breast. *Semin Nucl Med* 36:73-92, 2006
43. Ovadia D, Metser U, Lievshitz G, et al: Back pain in adolescents: Assessment with integrated <sup>18</sup>F-fluoride positron-emission tomography-computed tomography. *J Pediatr Orthop* 27:90-93, 2007
44. Lim R, Fahey FH, Drubach LA, et al: Early experience with fluorine-18 sodium fluoride bone PET in young patients with back pain. *J Pediatr Orthop* 27:277-282, 2007
45. Sterner T, Pink R, Freudenberg L, et al: The role of [<sup>18</sup>F]fluoride positron emission tomography in the early detection of aseptic loosening of total knee arthroplasty. *Int J Surg* 5:99-104, 2007
46. Tayama Y, Takahashi N, Oka T, et al: Clinical evaluation of the effect of attenuation correction technique on <sup>18</sup>F-fluoride PET images. *Ann Nucl Med* 21:93-99, 2007
47. Brix G, Lechel U, Glatting G, et al: Radiation exposure of patients undergoing whole-body dual-modality <sup>18</sup>F-FDG PET/CT examinations. *J Nucl Med* 46:608-613, 2005
48. Fahey FH, Palmer MR, Strauss KJ, et al: Dosimetry and adequacy of CT-based attenuation correction for pediatric PET: Phantom study. *Radiology* 243:96-104, 2007
49. Patlak CS, Blasberg RG, Fenstermacher JD: Graphical evaluation of blood-to-brain transfer constants from multiple-time uptake data. *J Cereb Blood Flow Metab* 3:1-7, 1983
50. Brenner W, Vernon C, Muzi M, et al: Comparison of different quantitative approaches to <sup>18</sup>F-fluoride PET scans. *J Nucl Med* 45:1493-1500, 2004